

Tailoring peptide conformational space with organic gas modifiers in TIMS-MS

Alyssa Garabedian¹ · Fenfei Leng^{1,2} · Mark E. Ridgeway³ · Melvin A. Park³ · Francisco Fernandez-Lima^{1,2}Received: 25 March 2018 / Revised: 6 April 2018 / Accepted: 9 April 2018
© Springer-Verlag GmbH Germany, part of Springer Nature 2018

Abstract

Recently, we showed the advantages of Trapped Ion Mobility Spectrometry for the study of kinetic intermediates of biomolecules as a function of the starting solvent composition (e.g., organic content and pH) and collisional induced activation. In the present work, we further characterize the influence of the bath composition (e.g., organic content) on the conformational space of an intrinsically disordered, DNA binding peptide: AT-hook 3 (Lys-Arg-Pro-Arg-Gly-Arg-Pro-Arg-Lys-Trp). Results show the dependence of the charge state distribution and mobility profiles by doping the solution and the bath gas with organic modifiers (e.g., methanol and acetone). The high resolving power of the TIMS analyzer allowed the separation of multiple IMS band per charge state, and their relative abundances are described as a function of the experimental conditions. The use of gas modifiers resulted in larger ion-neutral collision cross sections, with a direct correlation between the size of the modifier and the CCS differences. Conformational isomer inter-conversion rates were observed as a function of the trapping time. Different from solution experiments, a larger variety of organic gas modifiers can be used to tailor the peptide conformational space, since peptide precipitation is not a problem.

Keywords Trapped ion mobility mass spectrometry · Intrinsically disordered protein · HMGA2 · ATHP

Introduction

Mass spectrometry-based methods have increasingly become a complementary or alternative research tool for investigating the conformational space of biomolecules under a variety of conditions, including biologically relevant conditions. [6, 16, 19, 37, 40] Specifically, ion mobility spectrometry combined with mass spectrometry (IMS-MS) has the capability to perform separation and selection of gas-phase ions, from heterogeneous solutions. It provides insight into both stable and intermediate structures, allowing for a more dynamic view and native-like folding information, [21] while resembling solution structures (memory effect). [5, 15, 18, 22, 25, 33, 35, 36, 38] Previous studies from our group showed the

advantages of ESI-TIMS-MS for the study of kinetically trapped intermediates of biomolecules. [1–4, 10, 11, 15, 20, 24, 27, 29, 31] Relevant to this study, we presented the folding pathways between local, free energy minima of AT-hook peptide 3 (ATHP3) leading to multiple, stabilized conformations. [26] Protonation site, backbone relaxation and side-chain orientations were implicated in defining each structure. We have shown that the conformational space can be altered by introducing dopants into the TIMS cell for the case of flavin adenine dinucleotide. [20] Different from other experiments where gas modifiers are used to increase the analytical power of IMS by increasing the size of the collision partner or inducing higher order multi-pole interactions, [9, 13, 14, 23, 32, 39] in this project we focused on the influence of the microenvironment on the stabilization of the conformational space of biomolecules.

In the present work, a ten amino acid intrinsically disordered peptide, Lys-Arg-Pro-Arg-Gly-Arg-Pro-Arg-Lys-Trp, was studied using nanoESI-TIMS-MS as a function of starting solvent (e.g. organic content and pH), bath gas collision partner and time after desolvation. This study is the first to report on the use of TIMS gas modifiers to tailor the peptide conformational space.

✉ Francisco Fernandez-Lima
fernandf@fiu.edu

¹ Department of Chemistry and Biochemistry, Florida International University, Miami, FL 33199, USA

² Biomolecular Sciences Institute, Florida International University, Miami, FL 33199, USA

³ Bruker Daltonics Inc., Billerica, MA 01821, USA

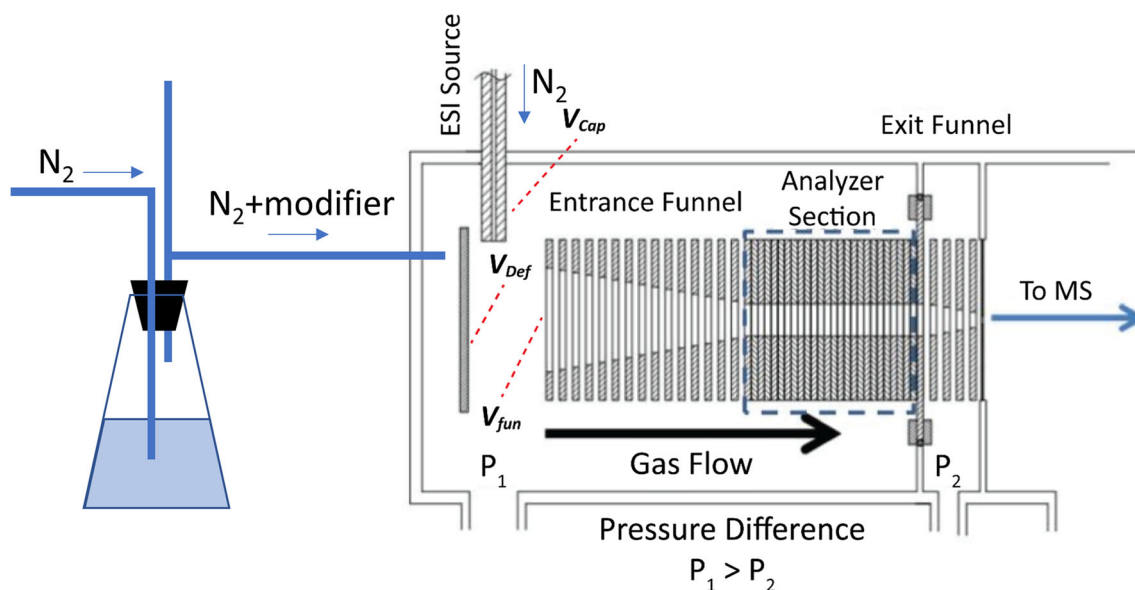


Fig. 1 Scheme utilized for the nESI-TIMS-MS experiments with organic gas modifiers. Notice that the gas velocity in the TIMS analyzer is kept constant

61 **Experimental methods**

62 **Materials and reagents** AT-hook peptides 3 (Lys-Arg-Pro-
 63 Arg-Gly-Arg-Pro-Arg-Lys-Trp) were purchased from
 64 Advanced ChemTech Inc. (Louisville, KY) and used as re-
 65 ceived. Methanol and acetone solvents, and ammonium ace-
 66 tate salts utilized in this study were analytical grade or better
 67 and purchased from Fisher Scientific (Pittsburgh, PA). A
 68 Tuning Mix calibration standard (G24221A) was obtained
 69 from Agilent Technologies (Santa Clara, CA) and used as
 70 received.

71 **Trapped ion mobility spectrometry – Mass spectrometry anal-**
 72 **ysis (TIMS-MS)** Details regarding the TIMS operation and spec-
 73 ifics compared to traditional IMS can be found elsewhere. [7,
 74 8, 12, 28, 30] Briefly, mobility separation in TIMS is based on
 75 holding the ions stationary against a moving gas using an
 76 electric field. The separation in a TIMS device can be de-
 77 scribed in the center of the mass reference frame using the
 78 same principles as in a conventional IMS drift tube. [17]
 79 Since mobility separation is related to the number of ion-
 80 neutral collisions (or drift time in traditional drift tube cells),
 81 the mobility separation in a TIMS device depends on the
 82 bath gas drift velocity, ion confinement and ion elution
 83 parameters. The reduced mobility, *K*, of an ion in a
 84 TIMS cell is described by:

$$K = \frac{v_g}{E} \approx \frac{A}{(V_{elution} - V_{out})}$$

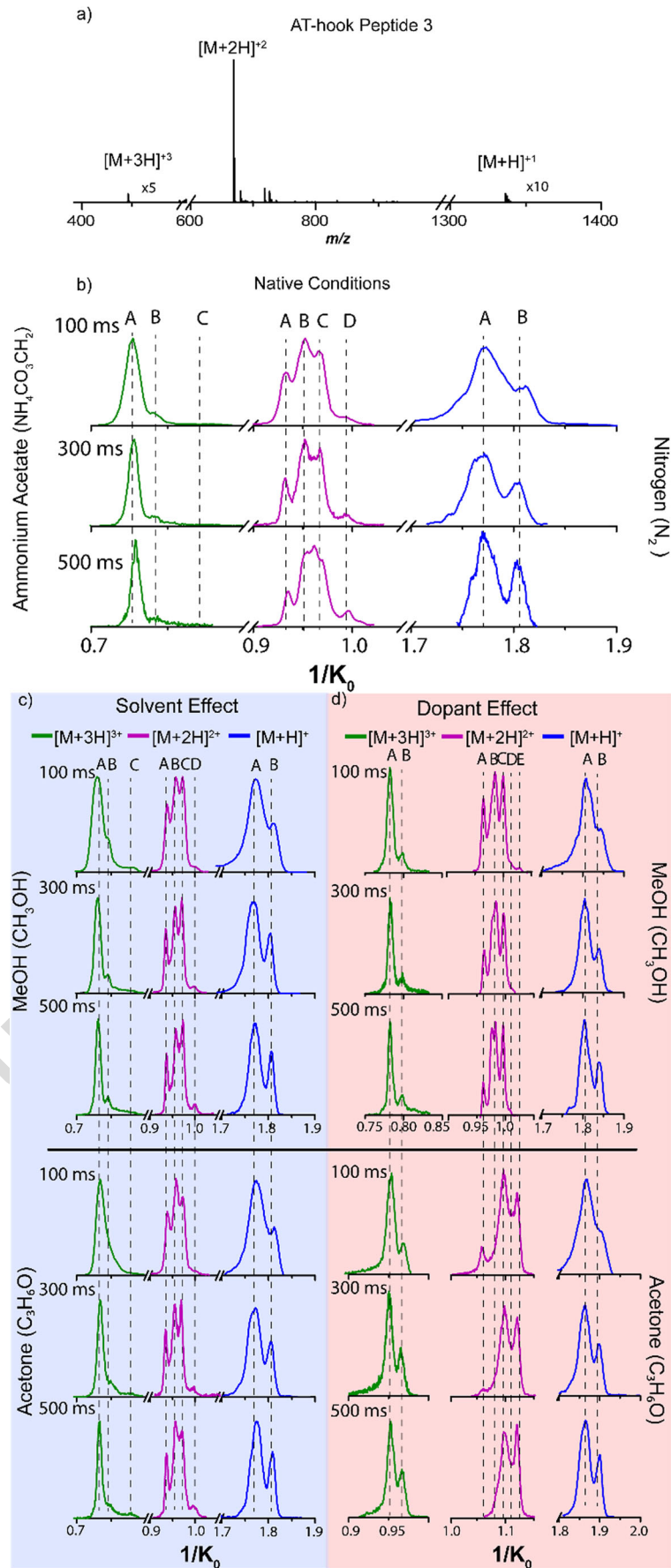
86 where v_g and *E* are the velocity of the gas and the applied
 87 electric field across the TIMS analyzer region. $V_{elution}$ is the
 88 voltage when the ions elute in the V_{ramp} sweep and V_{out} is the

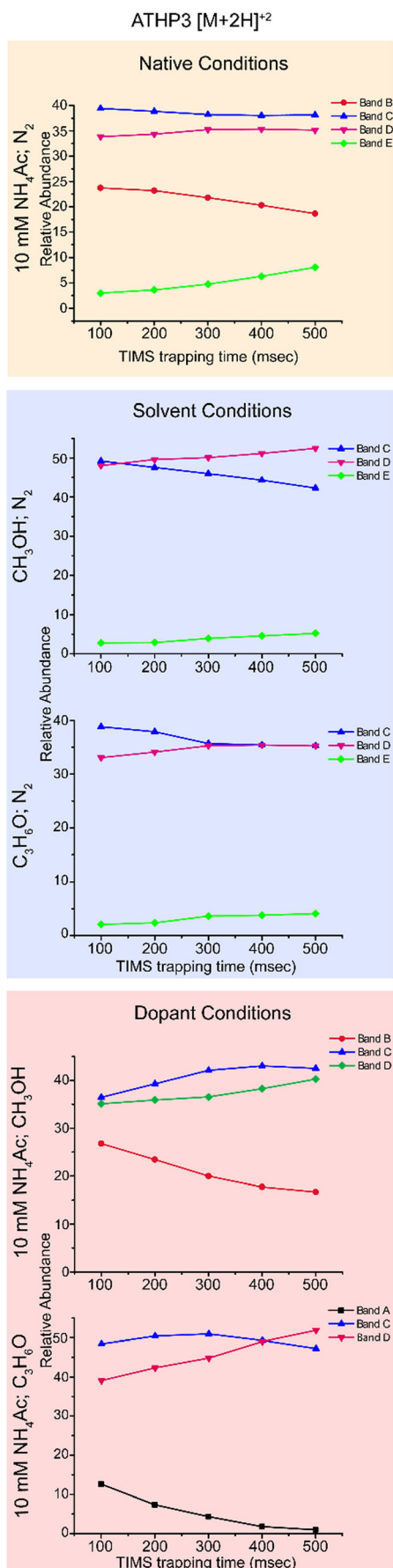
voltage applied at the end of the TIMS analyzer region. *A* is a
 89 constant that relates to the velocity of the bath gas and electric
 90 field axial distribution and can be calculated using mobility
 91 standards. Notice that, once *A* is calculated for a given bath
 92 gas (e.g., Tuning Mix as calibrants for N_2 bath gas), it will not
 93 change when using gas modifiers since the pressure difference
 94 between P_1 and P_2 are kept the same (see details in Fig. 1).
 95

A custom-built, pulled capillary nanoESI source was uti-
 96 lized for all the experiments. Quartz glass capillaries (O.D.:
 97 1.0 mm and I.D.: 0.70 mm) were pulled utilizing a P-2000
 98 micropipette laser puller (Sutter Instruments, Novato, CA) and
 99 loaded with 10 μ L aliquot of the sample solution. A typical
 100 nanoESI source voltage of \pm 600–1200 V was applied be-
 101 tween the pulled capillary tips and the TIMS-MS instrument
 102 inlet. Ions were introduced via a stainless steel tube ($1/16 \times$
 103 0.020", IDEX Health Science, Oak Harbor, WA) held at room
 104 temperature into the TIMS cell. It should be noted that all
 105 solvent studies were performed with nitrogen as the bath
 106 gas, and that all dopant experiments were conducted with
 107 peptides sprayed from 10 mM NH_4AC .
 108

Mobility calibration was performed using the Tuning Mix
 109 calibration standard (G24221A, Agilent Technologies, Santa
 110 Clara, CA) in positive ion mode (e.g., $m/z = 322$, $K_0 =$
 111 $1.376 \text{ cm}^2 \text{ V}^{-1} \text{ s}^{-1}$ and $m/z = 622$, $K_0 = 1.013 \text{ cm}^2 \text{ V}^{-1} \text{ s}^{-1}$).
 112 [12] The TIMS operation was controlled using in-house soft-
 113 ware, written in National Instruments Lab VIEW, and syn-
 114 chronized with the maXis Impact Q-ToF acquisition program.
 115 [7, 8] Gas modifiers were introduced at the entrance of the
 116

Fig. 2 a Typical mass spectra and (b) native IMS spectra of ATHP3 as a function of (c) starting solvent (methanol:H₂O or acetone:H₂O) or (d) dopant bath gas (methanol or acetone)





◀ **Fig. 3** The relative abundances of ATHP 3 $[M + 2H]^{2+}$ conformers as a function of the trapping time, stating solvent conditions and bath gas composition. Starting solvent and bath gas are listed to the left of the graphs

TIMS cell via vaporization of the respective solvents (e.g., 117
methanol or acetone) at a ratio of 2:1 air:air modified mix 118
(scheme shown in Fig. 1). For simplified mobility calibration, 119
the gas velocity was kept constant in all experiments (P1 and 120
P2 values). 121

Results and discussion 122

The analysis of ATHP3 peptide using nES-TIMS-MS resulted 123
in a charge state distribution of $[M + H]^+$ to $[M + 3H]^{3+}$. The 124
ATHP3 motif is mainly comprised of basic residues with sev- 125
en potential locations for protonation (e.g., N-terminus, four 126
arginines and two lysines), however, the most abundant ion 127
under all experimental conditions was the $[M + 2H]^{2+}$ 128
charge state (Fig. 2a). The mobility distributions observed 129
from our previous study of ATHP 3 $[M + 2H]^{2+}$ using 130
ESI-TIMS-MS are consistent with the current analysis 131
by nanoESI-TIMS-MS. [26] 132

At native conditions (Fig. 2b, pink mobility bands) ATHP3 133
 $[M + 2H]^{2+}$ populates four conformers (A-D). The mobility 134
bands are also conserved across the different organic solvent 135
conditions (Fig. 2c, pink mobility bands in blue panel). At 136
higher trapping times (e.g., 500 ms), a kinetically trapped 137
structure, and what we consider a more stable “desolvated” 138
conformer, appears between bands B and C of the native. The 139
presence of methanol in the TIMS cell did not alter the $[M +$ 140
 $2H]^{2+}$ conformers, while acetone significantly changed the 141
relative abundance and distribution of structures (Fig. 2d, 142
pink mobility band in pink panel). Three structures (A, B 143
and C) were observed for ATHP3 $[M + 3H]^{3+}$ over the range 144
of starting solvent solutions (Fig. 2b and c, green mobility 145
bands). Conformer A was the major structure present in all 146
experiments, followed by conformer B and C. The abundance 147
of conformer B, however, increased in the presence of acetone 148
in the TIMS cell. The mobility profiles of ATHP3 $[M + H]^+$ 149
showed the presence of two structures (A and B) which were 150
observed over the range of experimental conditions (Fig. 2b, c 151
and d, blue mobility bands). The distribution of ATHP 3 struc- 152
tures using acetone solvent cannot be recreated using acetone 153
in the TIMS cell. One possible explanation is that the differ- 154
ences in conformational space is due to interaction with the 155
ketone functional group of acetone. Unlike methanol’s alcohol 156
group, acetone’s ketone group can form various interactions 157
with the peptide, including 1) hydrogen bonding with the amide 158
of the peptide backbone, 2) disruption of hydrogen bonding 159
networks or, more likely, 3) dipole-dipole interactions with 160

161 the charged residues of the peptide. Confirming this explanation
162 will be the subject of future studies.

163 Changes in the conformational space as a function of the
164 trapping showed stabilization towards more energetically favored
165 structures as a function of the trapping time for $[M + H]^{+2}$
166 charge state (Fig. 3). While our measurements are only
167 sensitive to the 50–500 ms time scale, potential rearrange-
168 ments are possible in the first 50 ms after desolvation [34].
169 In the case of varying the starting solution (10 mM ammonium
170 acetate, and with methanol and acetone), a common trend in
171 the gas phase kinetics in nitrogen is the increase of the band E,
172 which corresponds to the largest CCS (and largest $1/K_0$) for
173 this charge state. However, in the case of gas modifiers, band
174 E is not observed, and the trends are best characterized by a
175 decrease of band B and band A for methanol and acetone,
176 respectively, which correspond to the smallest CCSs. We interpret
177 these results as the most stable gas-phase structures
178 tending to have larger CCSs than those initially observed in
179 solution. These effects may be a consequence of the absence
180 of the solvent, since in the gas-phase the lack of water molecules
181 promotes long range interactions. In the case of the
182 $[M + H]^+$ and $[M + H]^{+3}$ charge states, similar trends were
183 observed regarding the increase of larger CCS bands as a
184 function of the trapping time (see Fig. 2).

185 Conclusions

186 The results presented here displayed the utility of gas modifiers
187 in TIMS-MS for investigating and monitoring solution
188 versus gas-phase microenvironment contribution to the peptide
189 conformational space. When ionized from native conditions
190 (10 mM NH_4Ac and nitrogen bath gas), the mobility profiles
191 of ATHP 3 show an ensemble of conformers, which were
192 preserved as a function of increasing organic content
193 (methanol and acetone). Although the overall IMS profiles
194 were maintained, changes in the relative abundance of conformers
195 (e.g., conformational isomerization to the more stable gas-phase
196 structure) were observed and recorded. The inter-conversion
197 of structures, however, was small and often did not exceed
198 growth or decay abundances of ~10%. Comparison
199 between starting solvent and bath gas with the same organic
200 modifier showed that acetone as a dopant consistently
201 changed the original IMS profiles. Overall, we find evidence
202 for multiple stable conformers of these “disordered” motifs as
203 a function of starting solvent (e.g. organic content), bath gas
204 collision partner and time after desolvation. The sensitivity of
205 TIMS-MS allows for the observation of many low abundant
206 conformers, separation of closely related structures and tracking
207 of gas-phase stable structures via isomerization kinetics.
208 This methodology opens new avenues for the study of biomolecules
209 in the presence of gas modifiers that are not

accessible during solution experiments, due to the typical precipitation
210 of biomolecules during non-native conditions. 211

Acknowledgments This work was supported by the National Science
212 Foundation Division of Chemistry, under CAREER award CHE-
213 1654274, with co-funding from the Division of Molecular and Cellular
214 Biosciences to F.F.-L. The authors will also like to acknowledge the
215 helpful discussions and technical support from Dr. Mark E. Ridgeway
216 and Dr. Melvin A. Park from Bruker Daltonics Inc. during the develop-
217 ment and installation of the custom-built TIMS-TOF MS instrument. 218

References

1. Adams KJ, Montero D, Aga D, Fernandez-Lima F (2016) Isomer separation of polybrominated diphenyl ether metabolites using nanoESI-TIMS-MS. *Int J Ion Mobil Spectrom* 19(2-3):69–76. <https://doi.org/10.1007/s12127-016-0198-z> 221–224
2. Benigni P, Fernandez-Lima F (2016) Oversampling Selective Accumulation Trapped Ion Mobility Spectrometry Coupled to FT-ICR MS: Fundamentals and Applications. *Anal Chem* 88(14):7404–7412. <https://doi.org/10.1021/acs.analchem.6b01946> 225–228
3. Benigni P, Marin R, Fernandez-Lima F (2015) Towards unsupervised polyaromatic hydrocarbons structural assignment from SA-TIMS –FTMS data. *Int J Ion Mobil Spectrom*:1–7. <https://doi.org/10.1007/s12127-015-0175-y> 229–232
4. Benigni P et al (2016) Towards the analysis of high molecular weight proteins and protein complexes using TIMS-MS. *Int J Ion Mobil Spec* 19:95–104. <https://doi.org/10.1007/s12127-016-0201-8> 233–236
5. Chen S-H, Russell DH (2015) How closely related are conformations of protein ions sampled by IM-MS to native solution structures? *J Am Soc Mass Spectrom* 26(9):1433–1443 237–239
6. Feng X, Liu X, Luo Q, Liu B-F (2008) Mass spectrometry in systems biology: an overview. *Mass Spectrom Rev* 27(6):635–660. <https://doi.org/10.1002/mas.20182> 240–242
7. Fernandez-Lima FA, Kaplan DA, Park MA (2011a) Note: Integration of trapped ion mobility spectrometry with mass spectrometry. *Rev Sci Instrum* 82:126106 243–245
8. Fernandez-Lima FA, Kaplan DA, Suetering J, Park MA (2011b) Gas-phase separation using a Trapped Ion Mobility Spectrometer. *Int J Ion Mobil Spec* 14:93–98 246–248
9. Fernández-Maestre R, Wu C, Hill HH (2012) Buffer gas modifiers effect resolution in ion mobility spectrometry through selective ion-molecule clustering reactions. *Rapid Commun Mass Spectrom* 26(19):2211–2223. <https://doi.org/10.1002/rcm.6335> 249–252
10. Frost L, Baez MAM, Harrilal C, Garabedian A, Fernandez-Lima F, Leng F (2015) The dimerization state of the mammalian high mobility group protein AT-hook 2 (HMGA2). *PLoS One* 10(6):e0130478. <https://doi.org/10.1371/journal.pone.0130478> 253–256
11. Gonzalez WG, Ramos V, Diaz M, Garabedian A, Molano-Arevalo JC, Fernandez-Lima F, Miksovskaja J (2016) Characterization of the Photophysical, thermodynamic, and structural properties of the terbium (III)–DREAM complex. *Biochemistry* 55(12):1873–1886 257–260
12. Hernandez DR, DeBord JD, Ridgeway ME, Kaplan DA, Park MA, Fernandez-Lima FA (2014) Ion dynamics in a trapped ion mobility spectrometer. *Analyst* 139(8):1913–1921. <https://doi.org/10.1039/C3AN02174B> 261–264
13. Kafle A, Coy SL, Wong BM, Fomace AJ Jr, Glick JJ, Vouros P (2014) Understanding gas phase modifier interactions in rapid analysis by differential mobility-tandem mass spectrometry. *J Am Soc Mass Spectrom* 25(7):1098–1113. <https://doi.org/10.1007/s13361-013-0808-5> 265–268

- 270 14. Levin DS, Vouros P, Miller RA, Nazarov EG, Morris JC (2006) 325
271 Characterization of gas-phase molecular interactions on differential 326
272 mobility ion behavior utilizing an electrospray ionization- 327
273 differential mobility-mass spectrometer system. *Anal Chem* 78(1): 328
274 96–106. <https://doi.org/10.1021/ac051217k> 329
- 275 15. Liu FC, Kirk SR, Bleiholder C (2016) On the structural denatur- 330
276 ation of biological analytes in trapped ion mobility spectrometry - 331
277 mass spectrometry. *Analyst* 141(12):3722–3730. <https://doi.org/10.1039/C5AN02399H> 332
278 16. Loo JA (1997) Studying noncovalent protein complexes by 333
279 electrospray ionization mass spectrometry. *Mass Spectrom Rev* 334
280 16(1):1–23. [https://doi.org/10.1002/\(sici\)1098-2787\(1997\)16:](https://doi.org/10.1002/(sici)1098-2787(1997)16:1<1::aid-mas1>3.0.co;2-1) 335
281 [1<1::aid-mas1>3.0.co;2-1](https://doi.org/10.1002/(sici)1098-2787(1997)16:1<1::aid-mas1>3.0.co;2-1) 336
282 17. McDaniel EW, Mason EA (1973) Mobility and diffusion of ions in 337
283 gases. Wiley series in plasma physics. John Wiley and Sons, Inc., 338
284 New York 339
- 285 18. Meyer T, Gabelica V, Grubmüller H, Orozco M (2013) Proteins in 340
286 the gas phase. *Wiley Interdiscip Rev: Comput Mol Sci* 3:408–425 341
287 19. Miranker A, Robinson CV, Radford SE, Aplin RT, Dobson CM 342
288 (1993) Detection of transient protein folding populations by mass 343
289 spectrometry. *Science* 262(5135):896–900. [https://doi.org/10.1126/](https://doi.org/10.1126/science.8235611) 344
290 [science.8235611](https://doi.org/10.1126/science.8235611) 345
- 291 20. Molano-Arevalo JC, Hernandez DR, Gonzalez WG, Miksovskaja J, 346
292 Ridgeway ME, Park MA, Fernandez-Lima F (2014) Flavin adenine 347
293 dinucleotide structural motifs: from solution to gas phase. *Anal* 348
294 *Chem* 86(20):10223–10230. <https://doi.org/10.1021/ac5023666> 349
295 21. Pi J, Sael L (2013) Mass spectrometry coupled experiments and 350Q2
296 protein structure modeling methods. *Int J Mol Sci* 14:20635– 351
297 20657. <https://doi.org/10.3390/ijms141020635> 352
298 22. Pierson NA, Chen L, Valentine SJ, Russell DH, Clemmer DE 353
299 (2011) Number of solution states of bradykinin from ion mobility 354
300 and mass spectrometry measurements. *J Am Chem Soc* 133(35): 355
301 13810–13813. <https://doi.org/10.1021/ja203895j> 356
302 23. Porta T, Varesio E, Hopfgartner G (2013) Gas-phase separation of 357
303 drugs and metabolites using modifier-assisted differential ion mo- 358
304 bility spectrometry hyphenated to liquid extraction surface analysis 359
305 and mass spectrometry. *Anal Chem* 85(24):11771–11779. [https://](https://doi.org/10.1021/ac4020353) 360
306 doi.org/10.1021/ac4020353 361
307 24. Ridgeway ME, Silveira JA, Meier JE, Park MA (2015) 362
308 Microheterogeneity within conformational states of ubiquitin re- 363
309 vealed by high resolution trapped ion mobility spectrometry. 364
310 *Analyst* 140(20):6964–6972 365
311 25. Rosu F, Gabelica V, Joly L, Gregoire G, De Pauw E (2010) 366
312 Zwitterionic i-motif structures are preserved in DNA negatively 367
313 charged ions produced by electrospray mass spectrometry. *Phys* 368
314 *Chem Chem Phys* 12(41):13448–13454 369
315 26. Schenk ER, Ridgeway ME, Park MA, Leng F, Fernandez-Lima F 370
316 (2013) Isomerization kinetics of AT hook Decapeptide solution 371
317 structures. *Anal Chem* 86(2):1210–1214. [https://doi.org/10.1021/](https://doi.org/10.1021/ac403386q) 372
318 [ac403386q](https://doi.org/10.1021/ac403386q) 373
319 27. Schenk ER, Mendez V, Landrum JT, Ridgeway ME, Park MA, 374
320 Fernandez-Lima F (2014a) Direct observation of differences of ca- 375
321 rotenoid polyene chain cis/trans isomers resulting from structural 376
322 topology. *Anal Chem* 86(4):2019–2024. [https://doi.org/10.1021/](https://doi.org/10.1021/ac403153m) 377
323 [ac403153m](https://doi.org/10.1021/ac403153m) 378
324 28. Schenk ER, Mendez V, Landrum JT, Ridgeway ME, Park MA, 379
325 Fernandez-Lima FA (2014b) Direct observation of differences of 380
326 carotenoid polyene chain cis/trans isomers resulting from structural 381
327 topology. *Anal Chem* 86(4):2019–2024. [https://doi.org/10.1021/](https://doi.org/10.1021/ac403153m) 382
328 [ac403153m](https://doi.org/10.1021/ac403153m) 383
329 29. Schenk ER, Ridgeway ME, Park MA, Leng F, Fernandez-Lima F 384
330 (2014c) Isomerization kinetics of AT hook decapeptide solution 385
331 structures. *Anal Chem* 86(2):1210–1214. [https://doi.org/10.1021/](https://doi.org/10.1021/ac403386q) 386
332 [ac403386q](https://doi.org/10.1021/ac403386q) 387
333 30. Schenk ER, Ridgeway ME, Park MA, Leng F, Fernandez-Lima FA 388
334 (2014d) Isomerization kinetics of AT hook Decapeptide solution 389
335 structures. *Anal Chem* 86(2):1210–1214. [https://doi.org/10.1021/](https://doi.org/10.1021/ac403386q) 390
336 [ac403386q](https://doi.org/10.1021/ac403386q) 391
337 31. Schenk ER, Almeida R, Miksovskaja J, Ridgeway ME, Park MA, 392
338 Fernandez-Lima F (2015) Kinetic intermediates of holo- and apo- 393
339 myoglobin studied using HDX-TIMS-MS and molecular dynamic 394
340 simulations. *J Am Soc Mass Spectrom* 26(4):555–563. [https://doi.](https://doi.org/10.1007/s13361-014-1067-9) 395
341 [org/10.1007/s13361-014-1067-9](https://doi.org/10.1007/s13361-014-1067-9) 396
342 32. Schneider B, Covey T, Nazarov E (2013) DMS-MS separations 397
343 with different transport gas modifiers vol 16. [https://doi.org/10.](https://doi.org/10.1007/s12127-013-0130-8) 398
344 [1007/s12127-013-0130-8](https://doi.org/10.1007/s12127-013-0130-8) 399
345 33. Seo J, Hoffmann W, Wamke S, Bowers MT, Pagel K, von Helden G 400
346 (2016) Retention of native protein structures in the absence of sol- 401
347 vent: a coupled ion mobility and spectroscopic study. *Angew Chem* 402
348 *Int Ed* 55(45):14173–14176. [https://doi.org/10.1002/anie.](https://doi.org/10.1002/anie.201606029) 403
349 [201606029](https://doi.org/10.1002/anie.201606029) 404
350 34. Shelimov KB, Jarrold MF (1997) Conformations, unfolding, and 405
351 refolding of Apomyoglobin in vacuum: an activation barrier for 406
352 gas-phase protein folding. *J Am Chem Soc* 119(13):2987–2994. 407
353 <https://doi.org/10.1021/ja962914k> 408
354 35. Shi L, Holliday AE, Glover MS, Ewing MA, Russell DH, Clemmer 409
355 DE (2016) Ion mobility-mass spectrometry reveals the energetics of 410
356 intermediates that guide Polyproline folding. *J Am Soc Mass* 411
357 *Spectrom* 27(1):22–30 412
358 36. Silveira JA, Fort KL, Kim D, Servage KA, Pierson NA, Clemmer 413
359 DE, Russell DH (2013) From solution to the gas phase: stepwise 414
360 dehydration and kinetic trapping of substance P reveals the origin of 415
361 peptide conformations. *J Am Chem Soc* 135(51):19147–19153. 416
362 <https://doi.org/10.1021/ja4114193> 417
363 37. Simoneit BRT (2005) A review of current applications of mass 418
364 spectrometry for biomarker/molecular tracer elucidations. *Mass* 419
365 *Spectrom Rev* 24(5):719–765. <https://doi.org/10.1002/mas.20036> 420
366 38. Voronina L, Masson A, Kamrath M, Schubert F, Clemmer D, 421
367 Baldauf C, Rizzo T (2016) Conformations of prolyl-peptide bonds 422
368 in the bradykinin 1–5 fragment in solution and in the gas phase. *J* 423
369 *Am Chem Soc* 138(29):9224–9233. [https://doi.org/10.1021/jacs.](https://doi.org/10.1021/jacs.6b04550) 424
370 [6b04550](https://doi.org/10.1021/jacs.6b04550) 425
371 39. Waraksa E, Gaik U, Namieśnik J, Sillanpää M, Dymerski T, 426
372 Wójtowicz M, Puton J (2016) Dopants and gas modifiers in ion 427
373 mobility spectrometry vol 82. [https://doi.org/10.1016/j.trac.2016.](https://doi.org/10.1016/j.trac.2016.06.009) 428
374 [06.009](https://doi.org/10.1016/j.trac.2016.06.009) 429
375 40. Winston RL, Fitzgerald MC (1997) Mass spectrometry as a readout 430
376 of protein structure and function. *Mass Spectrom Rev* 16(4):165– 431
377 179. [https://doi.org/10.1002/\(sici\)1098-2787\(1997\)16:4<165::aid-](https://doi.org/10.1002/(sici)1098-2787(1997)16:4<165::aid-mas1>3.0.co;2-f) 432
378 [mas1>3.0.co;2-f](https://doi.org/10.1002/(sici)1098-2787(1997)16:4<165::aid-mas1>3.0.co;2-f) 433
379 380

AUTHOR QUERIES

AUTHOR PLEASE ANSWER ALL QUERIES.

- Q1. Please check reference entry if captured and presented correctly.
- Q2. Please check provided volume, Issue and page numbers if correct.

UNCORRECTED PROOF